

# RF Frontend for a Full Duplex Radar Platform

Gavin T. Watkins, Vianney Anis, Fred Wiffen

## Abstract

Full-duplex (FD) or simultaneous transmit and receive (STAR) allows the reception of one signal while simultaneously transmitting another on the same frequency and timeslot. Previously this technique has been proposed for wireless networks and mobile communications. This work considers applying Self-Interference Cancellation (SiC) technology to an X-band weather radar to allow the reception of a return echo during the transmission pulse, thereby reducing the minimum target range. Specifically, the development of an RF frontend testbed to verify the concept is discussed in this paper. The RF frontend up- and down-converts a 50 MHz intermediate frequency (IF) to 9.45 GHz in two-stages with an intermediate IF of 2.4 GHz. The design, simulation, and production of the 9.45 GHz RF SiC and IF filters are presented. The complete system including converters and RF SiC reduced the Self-interference (Si) power to -59.8 dBm when using 10 dBm transmit power, a realistic horn antenna and a 1.63 MHz bandwidth radar frequency modulated continuous wave (FMCW) chirp pulse.

## Introduction

Accurate weather forecasting has become increasingly important as the impact of climate change has resulted in more extreme weather variation. In some parts of the world this has led to natural disasters with a devastating impacts on human life and infrastructure **Error! Reference source not found..** One method of forecasting is weather radar whereby a radar system tracks water droplet, i.e. cloud formations and precipitation [2]. One challenge is that cloud formations need to be tracked over a great distance – up to 60 km for an X-band radar – and at close range. Radars operate by transmitting a pulse of high frequency RF energy and then detecting the returned echo from a target. The maximum range ( $R_{max}$ ) achievable is determined by several factors, including antenna gain (G), transmit power ( $P_s$ ), radar cross section of the target ( $\sigma$ ), signal wavelength ( $\lambda$ ), length of transmit pulse ( $t_i$ ) and minimum receive power ( $P_{Emin}$ ), as shown in equation (1):

$$R_{max} = \sqrt[4]{\frac{P_s G^2 \lambda^2 \sigma t_i}{P_{Emin} (4\pi)^3}} \quad (1)$$

Many of these factors are fixed, for example:  $P_s$  (regulation), G (cost) and  $\sigma$  of clouds (nature).  $t_i$  also has an influence as a longer pulses contain more energy, but limit the minimum target range. This is because the transmit pulse power is significantly greater than the received signal, so reception of an echo is difficult during transmission. In the system discussed here, the transmit pulse length is 36  $\mu$ s, resulting in a minimum target distance of 6 km allowing for rise and fall times of 5  $\mu$ s.

Two common solutions exist for allowing echoes from targets closer than 6 km to be received: transmitting a short pulse and a long pulse on two different frequency channels **Error! Reference source not found.** or transmitting a short pulse and then a long pulse in two different timeslots **Error! Reference source not found.** as shown in Fig. 1 (a) and (b) respectively. The first solution requires two complete transmit and receive chains increasing cost, and two transmission licenses increasing operating cost (OPEX). The second solution results in slower imaging of a target. A third

solution, presented in this paper, is to use FD techniques whereby a weak signal can be received in the presence of a transmission on the same frequency band in the same time slot.

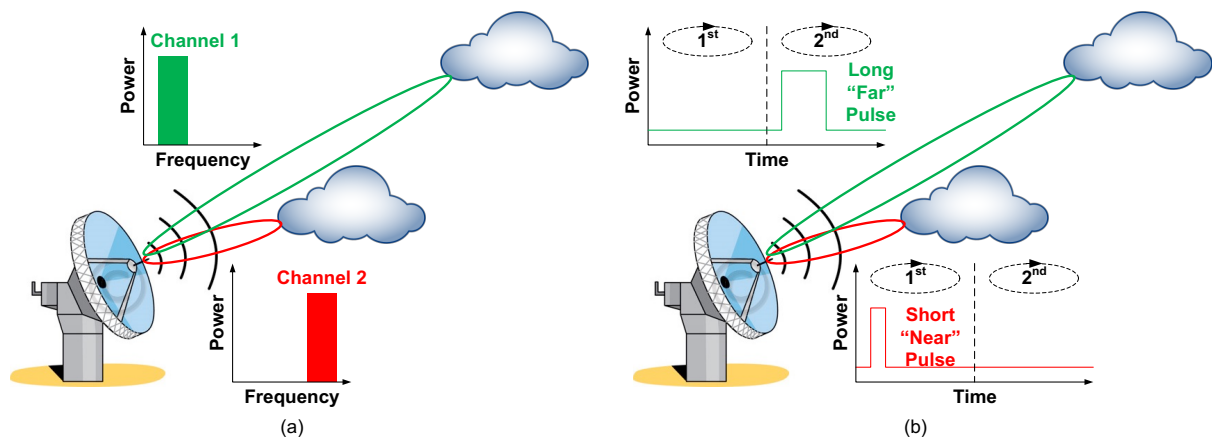


Fig. 1: (a) A radar operating on two different frequency channels, (b) radar operating on two different time slots

### Full Duplex Weather Radar

Most FD or STAR techniques cancel the transmitted Si signal in the receive path by tapping off a small portion of the transmit signal and injecting it into receive path in anti-phase to the Si with equal amplitude. Further, a combination of RF and digital/baseband SiC **Error! Reference source not found.** is used. The RF effectively applies a coarse cancellation and the digital a finer level. Essentially, the RF SiC reduces the Si to a level whereby it does not overload the sensitive receiver where distortion would be produced, or potentially damaging the receiver. A simplified schematic of an FD radar platform to verify the principle is shown in Fig. 2.

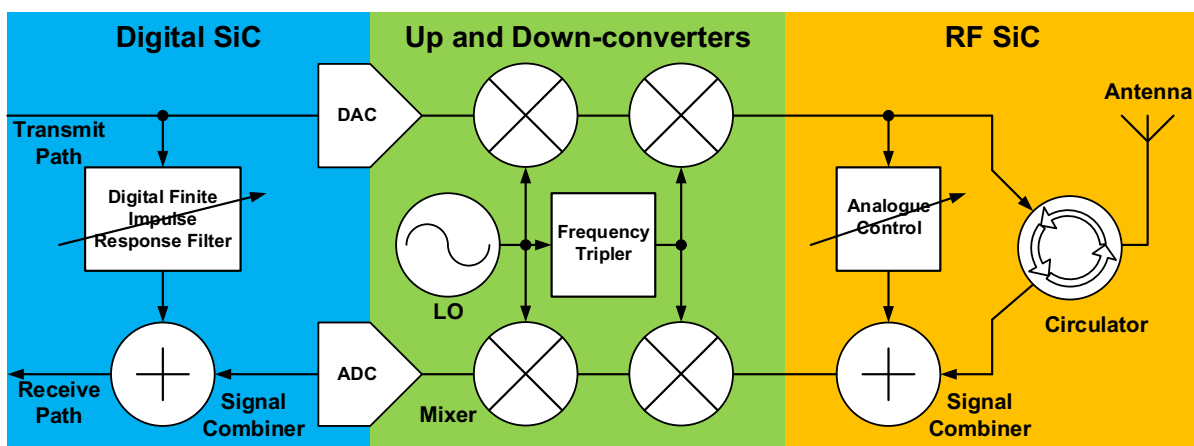


Fig. 2: Simplified schematic for platform

The antenna – which here is a Flann DP240 horn antenna – is coupled to the transmit and receive paths with a circulator. Some FD systems designed for low cost wireless communications uses hybrid couplers [6], but these incur 3 dB loss to both transmit and receive path. This is unacceptable for a radar system with 100 W transmit power and a very low noise figure receive path. In Fig. 2, a portion of the transmitted signal is tapped off before the circulator with a directional coupler. It's gain and

phase are manipulated with a variable attenuator (A) and phase shifter ( $\theta$ ) before injection into the received path to cancel the  $S_i$ .

Connected to the RF SiC are the up- and down-converters. A dual conversion architecture converts the 50 MHz digital IF to X-band – 9.45 GHz specifically. An intermediate IF of 2.4 GHz was chosen so that a common local oscillator (LO) of 2.35 GHz could be used. This is tripled to produce 7.05 GHz for the higher conversion. Most of the frequency converter is implemented with off-the-shelf components apart from custom bandpass filters as none were available at the time.

The digital SiC is implemented on a Xilinx ZCU102 FPGA evaluation board where a portion of the transmitted signal is manipulated with an adaptive Finite Impulse Response (FIR) filter and injected into the received path. ADS5263 ADCs and DAC37J82 DACs on evaluation modules running at 100 and 400 MSps respectively interface the analogue to digital parts. Several designs are currently under consideration for the digital SiC, with designs based on least mean square (LMS) and recursive least square algorithms in fractionally spaced and parallel Hammerstein structures. The design of the digital section will be dealt with more in depth in a future publication [7].

### RF SiC

For the platform described in this paper, the transmit power is reduced from 100 W (50 dBm) to 10 mW (10 dBm). This allows SiC at X-band to be demonstrated without incurring the cost or potential hazards of transmitting 50 dBm at 9.45 GHz. The Toshiba’s FD weather radar is based on a dual receiver paths per polarisation architecture to meet the dynamic range requirements: a Near Path (0-6 km) and a Far Path (6-60 km). Both paths are coupled to the receive path with a 16 dB coupler as shown in Fig. 3 (a), however, FD only need be applied to the Near Path. This also shows the relative powers around the circuit for a target  $-40$  dBm  $S_i$  power in the Near Path.

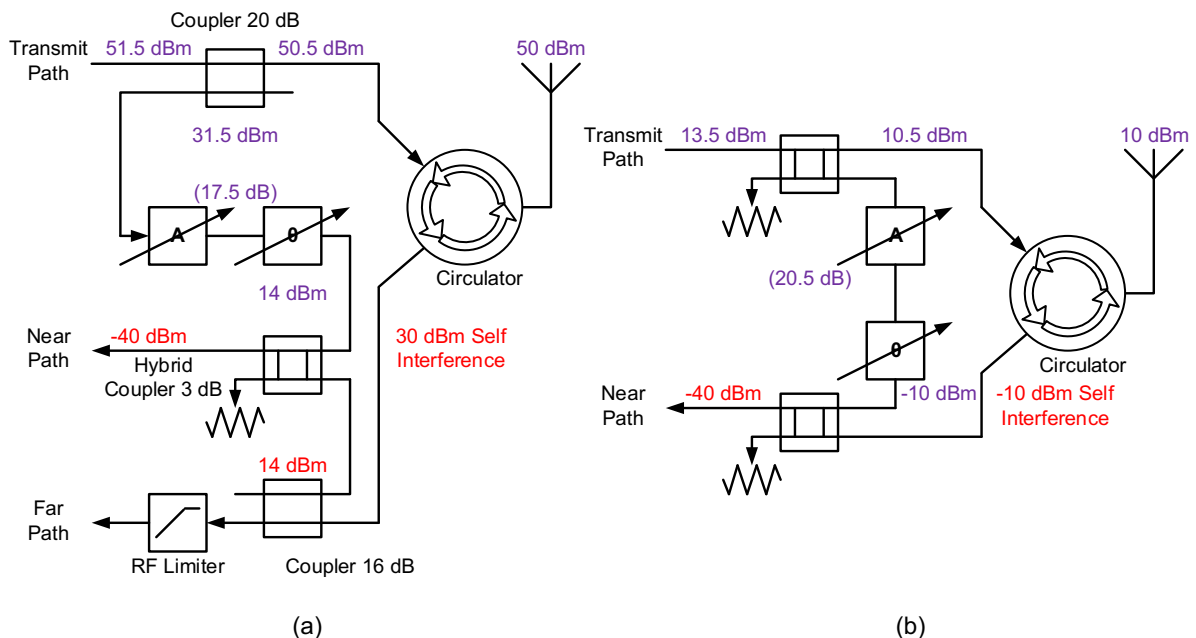


Fig. 3: Detailed FD schematics: (a) original dual path architecture and (b) Near Path only for the testbed.

As this platform has a lower transmit power and is for demonstrates the FD principle, only the Near Path is implemented as shown in Fig. 3 (b). For the reduced transmit power and the lack of efficiency requirements, the transmitter reference signal is tapped off with a 3 dB hybrid coupler. This design exclusively uses hybrid couplers, including A and  $\theta$  – which are based on hybrid couplers [7] – used for manipulating the reference signal which cancels the Si. With the reduced transmit power, the RF SiC requirements are reduced compared to the design in Fig 3 (a). For example, it is assumed that the Si power due to the circulator and antenna mismatch is -10 dBm. Therefore, the RF SiC only need provide an additional -30 dB SiC to meet the -40 dBm requirement, or -50 dB relative to the transmitted signal. Fig. 3(a) would require an additional -20 dB SiC making -70 dB in total.

The designs of A and  $\theta$  are critical as they must cover the required ranges with sufficient resolution for the reference and Si signals to combine destructively. For example, to achieve -60 dB the gain and phase imbalance must be no greater than 0.01 dB and 0.01° respectively **Error! Reference source not found.** This must also be maintained over the total signal bandwidth which is in this work is 1.63 MHz. For this demonstrator the RF SiC need only provide -30 dB of SiC, therefore requiring a gain and phase imbalance no greater than 0.2 dB and 0.2° over the signal bandwidth.

At X-band, stray parasitic capacitance and inductance can have a large effect. To reduce their impact, small – in value and physical dimensions – tuning elements are required for A and  $\theta$ . For this work MAT-N25 PIN diodes and SMV1408-040 varactor diodes were used in A and  $\theta$  respectively. A combined attenuator and phase shifter was designed in Microwave Office (MWO) and simulated resulting in the tuning range shown in Fig. 4.

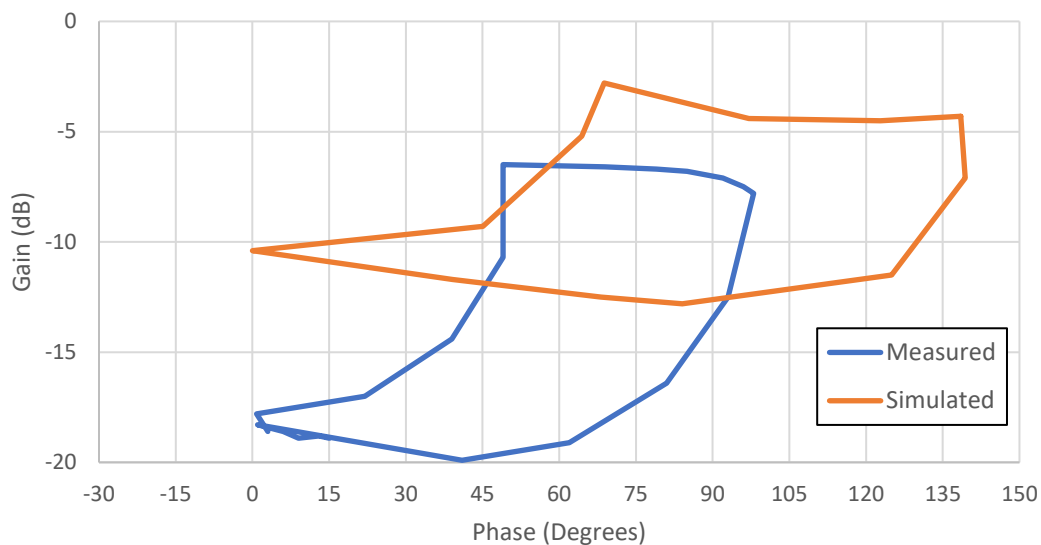


Fig. 4: Simulated and measured results for gain and phase elements

The simulated combined A and  $\theta$  have a phase range of 138° and gain range of 10 dB at 9.45 GHz. This range can be shifted with the addition of delay lines and attenuator pads to complement the Si. When fabricated on 0.5 mm Taconic TLY-5 substrate the measured response was shifted as also shown in Fig. 4. This and all PCBs in this work were manufactured with a LPKF PCB router. The measured result has a reduced phase range of 97°, but an increased gain range of 14.4 dB. This large difference is due to the simplified nature of the PIN and varactor diode models which consisted only of passive components extracted from the datasheet. The combined simulated A and  $\theta$  was then incorporated in the simulation model for the whole RF SiC shown in Fig. 5.

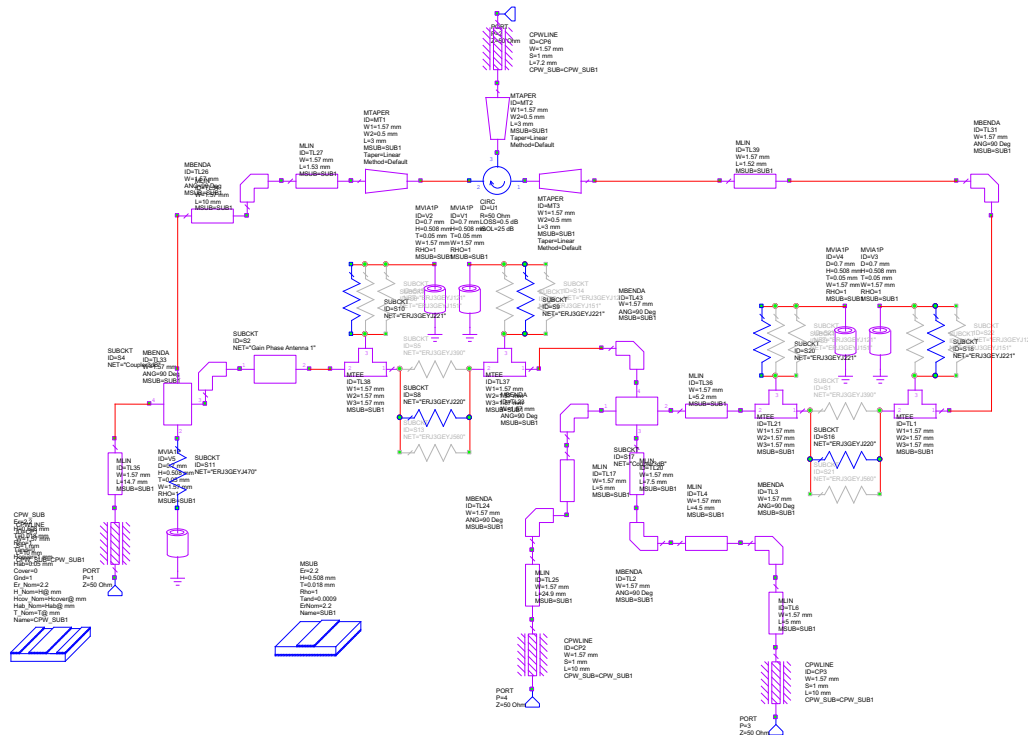


Fig. 5: MWO simulation model of RF SiC

The RF SiC is designed as a self-contained unit with additional attenuator pads and delay lines to allow course tuning of the SiC during construction. The Flann Horn was measured on a VNA and its S-parameters imported into the simulation. It exhibited significant ripple over its wide (2 GHz to 18 GHz) operating band due to different modes being excited. Its response impacts the simulated SiC as shown in Fig. 6 where when terminated with a 50  $\Omega$  -98.6 dB is achieved, but only -87.1 dB with the horn antenna. A similar difference was found for the practical SiC where -84.4 dB SiC was possible with a 50  $\Omega$  load, but only -66.1 dB with the horn antenna. An anechoic chamber was not available when measuring the horn, but it was surrounded with radio absorbing material (RAM) to reduce reflection (radar clutter) from the surrounding room.

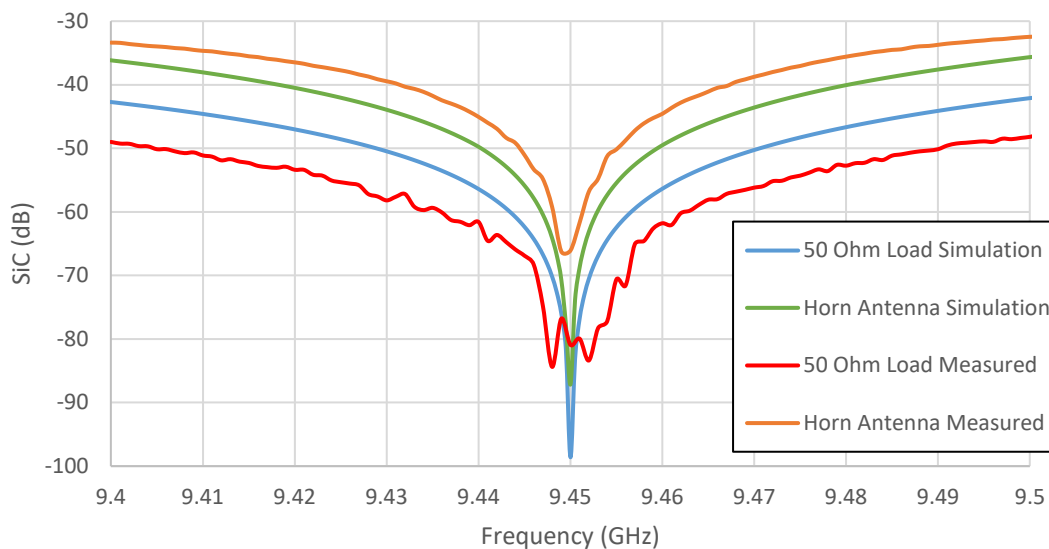


Fig. 6: Simulated and measured sweeps of RF SiC at 9.45 GHz

## Frequency Conversion

As previously mentioned, two levels of frequency up-conversion are used to get from 50 MHz to 9.45 GHz, and two levels of down-conversions back down to 50 MHz with an intermediate IF of 2.4 GHz. This arrangement is suboptimal as the first conversion has an image frequency at 2.3 GHz which is hard to filter. A bandpass (BP) filter with a Q of  $>12$  is required for this which can be difficult to realise with microstrip. However, this demonstrator operates in ideal conditions so it not susceptible to external interference which could exist at the image frequencies. The BP filter for the first IF were edge coupled type on 0.8 mm FR4 substrate. The main limitation on filter performance are manufacturing tolerances and substrate consistency. With the LPKF router the minimum reliable PCB track gap is 0.1 mm. The built-in filter wizard of Qucs (an open source RF simulation tool) was first used to design the BP filter, which was then electromagnetic (EM) simulated in MWO. The resulting filter had a 2.0 dB simulated insertion loss and a -3dB passband from 2.45 GHz to 2.62 GHz. A practical filter was fabricated which had an increase insertion loss of -5.4 dB and a -3 dB passband of 2.39 GHz to 2.55 GHz when fitted with a metal screening can. This was combined with an ADE-35+ Minicircuits mixers and ZX60-43-S+ Minicircuits amplifiers to produce the converter response shown in Fig. 7 when transmit and receiver converters were connected together in a back-to-back loop test so that the input and output were the same frequency.

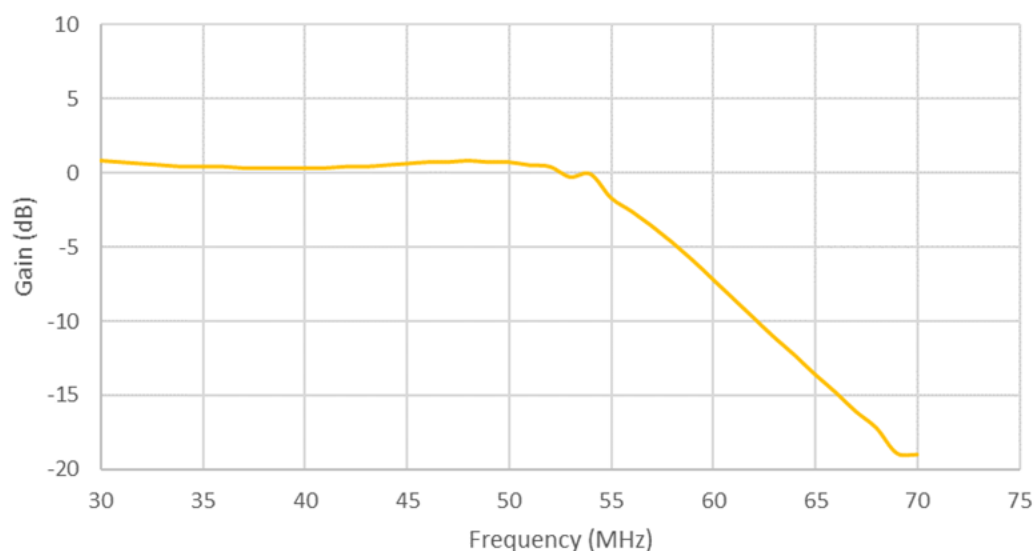


Fig. 7: Measured back-to-back loop test of first converter

The response shown in Fig. 7 shows a lowpass response with a -3 dB bandwidth of 56 MHz, sufficient for the 1.63 MHz FMCW radar signal. The up- and down- converters were built in a diecast aluminium box with individual screening cans for the filters and RAM to reduce leakage.

The second converter from 2.4 GHz to 9.45 GHz has an image response at 4.65 GHz ( $7.05 \text{ GHz} - 2.4 \text{ GHz}$ ) which is easier to filter. An edge coupled filter was again developed using the design flow discussed above and fabricated on 0.5 mm TLY-5 substrate. The simulated filter had an insertion loss of 0.5 dB and a -3dB passband of 8.94 GHz to 10.13 GHz. Practically, the insertion loss was 1.6 dB at 9.45 GHz and a -3 dB passband of 8.75 GHz to 9.75 GHz. These were housed in individually screened metal cans as were Wilkinson splitter and combiners. Connectorized Minicircuits ZX60-123LN-S+ amplifiers and ZX05-14-S+ mixers completed the second converter. The total response of both transmit and receiver converters from 50 MHz to 9.45 GHz and back to 50 MHz is shown in Fig. 8.

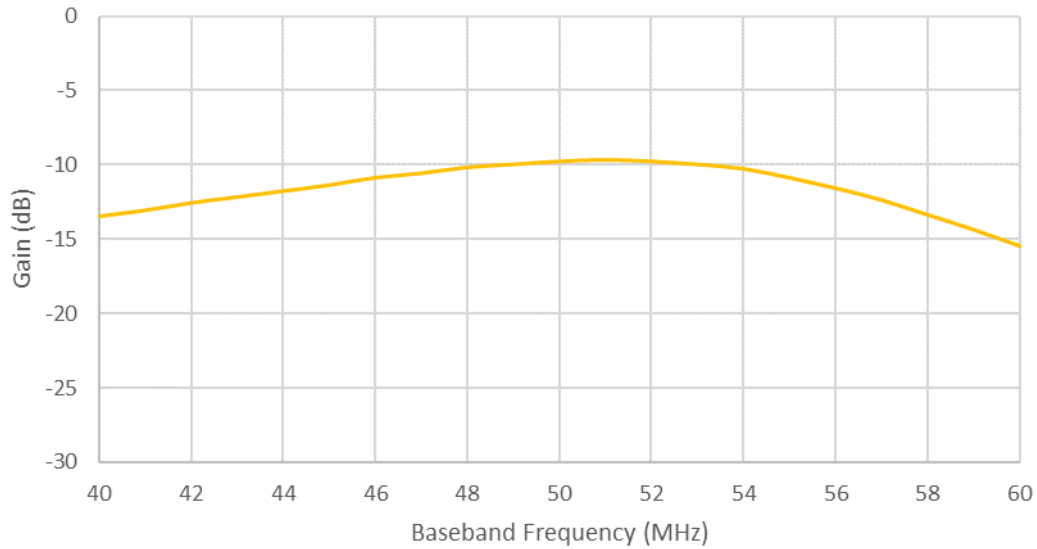


Fig.8: Measured back-to-back loop test of first and second converters

### Hardware Prototype

A full prototype was constructed based on the system elements discussed above. This was housed in a 19-inch rack case as shown in Fig. 9. The prototype in Fig. 9 is for a dual polarisation (horizontal and vertical) version, however a common transmit channel is shared between the two channels. The dual channel prototype will be described in the future paper [7]. On the front panel four multiturn potentiometers control both  $A$  and  $\theta$  for each channel. The final prototype will also include a switch to select either the front panel controls or digital-to-analogue converters in the digital baseband. The horn antenna is underneath the prototype with RAM in front of it. A Keysight N5172B provides the 2.35 GHz LO signal, from which the 7.05 GHz LO is also derived. The 50 MHz input radar pulses are generated off-line in Python and uploaded to a Tektronix AFG3101 arbitrary waveform generator.

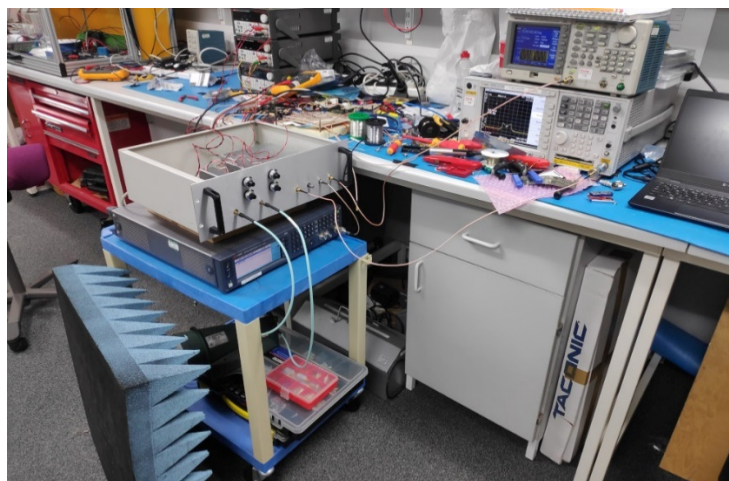


Fig: 9. photograph of total system

## System Results

The FMCW radar chirp also had rise- and fall-times of 5  $\mu\text{s}$  to shape the pulse in the frequency domain, thereby reducing out-of-band emissions. Fig. 10 shows the radar pulse in the time domain when the system is detuned – i.e. FD disabled – with a 50  $\Omega$  load on the antenna port and with the horn antenna attached. The transmit power at the antenna port was 10 dBm as in Fig. 3 (b).

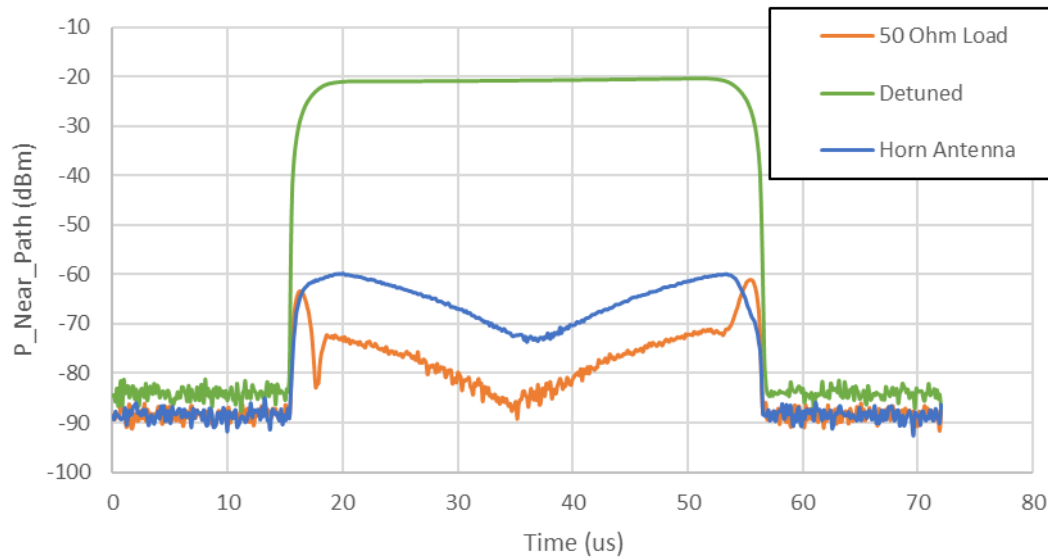


Fig.10: Overall RF results with FMCW chirped radar pulse

The SiC has a characteristic notch shape due to the frequency sweeping nature of the chirp between 9.449185 GHz and 9.450815 GHz. This is indicated in Fig. 6 where high SiC is only achieved over a narrow bandwidth. With a 50  $\Omega$  load attached the maximum received power is -61.1 dBm with 10 dBm transmit power. This is well below the -40 dBm specified in Fig. 3. It will be noted that there are “horns” present on the 50  $\Omega$  load trace during the rise- and fall-times. These are due to a non-linear gain or phase response in either the circulator or A and  $\theta$  paths in the RF SiC resulting in sub-optimum cancellation. With the horn antenna this is degraded to a maximum of -59.8 dBm, which still meets the target.

## Conclusion

The RF section of a FD X-band weather radar testbed is described in this paper. It consists of an RF SiC and two frequency conversion stages for the transmit and receive channels. FD allows the radar to receive an echo during the transmit pulse phase to reduce the minimum target range while still being able to image targets (precipitation) up to 60 km away. The RF SiC achieved -87.1 dB in simulation with a model of a horn antenna and -66.0 dB practically with the antenna connected. When incorporated with the frequency converters, the resulting maximum Si power in the testbed was -59.8 dBm with the horn antenna and 10 dBm transmit power, below the required -40 dBm target.



## References

- [1] "Japan earthquake and tsunami of 2011", *Encyclopaedia Britannica*, pub. online, accessed 14/01/2022.
- [2] "Weather Radar", *Wikipedia*, pub online, accessed 14/01/2022.
- [3] W. Lei, M. Wang, H. Huang, Y. Lv, H. Yu, "Dual-channel consistency analysis of dual-polarized weather radar based on light rain algorithm", *2019 International Conference on Meteorology Observations (ICMO)*, 28-31 Dec.
- [4] Furuno Electric co, patent WO2017145588A1, "Radar device and radar image generating method".
- [5] D. Bharadia, E. McMillin, S. Katti, "Full duplex radios" *SIGCOMM'13*, Aug. 12–16, 2013, pp. 375-386.
- [6] G. T. Watkins, "Single Antenna Full Duplex Communications Using Variable Impedance Network", *Microwave Journal*, August 2021.
- [7] V. Anis, F. Wiffen, G. Watkins, S. Jardak, "On the Feasibility of Full-Duplex in Dual-Polar X-band Weather Radars", in production
- [8] "Reflection Attenuators", online at [www.Microwaves101.com](http://www.Microwaves101.com).
- [9] G. T. Watkins, "A tuneable rat-race coupler for full duplex communications", *International Journal of Microwave and Wireless Technologies*, 26<sup>th</sup> May, 2021, pp. 1-7.